ITERATION THEORY (ECIT '02)
J. Sousa Ramos, D. Gronau, C. Mira,
L. Reich, A. Sharkovsky (Eds.)
Grazer Math. Ber., ISSN 1016–7692
Bericht Nr. 346 (2004), 1-18

Transition from a smooth basin boundary to a fractal one in a class of two-dimensional endomorphisms

Anna Agliari, Laura Gardini and Christian Mira

Abstract

This paper is devoted to the study of a family of two-dimensional noninvertible maps, depending on two parameters. The family is topologically semiconjugated to the complex quadratic map Z for a particular parameter value. The variation of this parameter value permits a full identification of one of the possible bifurcation mechanisms leading to the fractalization of a basin boundary from a smooth situation. It will be shown that the bifurcations occurring at the points on this boundary have the fractal structure of *box-within-a-box* type generated by the one-dimensional Myrberg's map $x' = x^2 - c$. Besides the transition of a *smooth* boundary *to* a *fractal* one, it will be shown also one example of transition from a *fractal* boundary to an *half fractal* one. This last transition occurs due to the existence of smooth arcs which recur in a fractal way in the boundary of a simply connected basin.

1 Introduction

Some bifurcation mechanisms leading to a fractal basin boundary generated by a two-dimensional noninvertible map has been already considered in Agliari et al. 2003 and references therein. The present paper considers a simpler form of maps family, which makes more transparent the transition to a fractal basin boundary.

The two-dimensional noninvertible map considered here is given by

$$T : \begin{cases} x' = x^2 + y - c \\ y' = \gamma y + 4x^2 y \end{cases} \tag{1}$$

T divides the plane into three regions: Z_i, $i = 0, 2, 4$, a point of Z_i having i real rank-one preimages (Mira et al. 1994, 1996,a,b). Inside Z_i the plane can be considered as made up of i sheets, each one being related to a well defined rank-one preimage, this constituting the *(Riemann) foliation* of the plane (see Gumowski and Mira 1980, Mira et al. 1996a,b, Abraham et al. 1997). Two sheets join at a critical curve LC, separating the regions Z_i, and locus of points having two coincident preimages on the curve LC_{-1}, $T(LC_{-1}) = LC$. In the case of a smooth map such as T, LC_{-1} is defined by $|J| = 0$, where $|J|$ denotes the Jacobian determinant of the map.

Mathematics Subject Classification 2000: 37E99, 37G99.
Keywords and phrases: dynamical system, two-dimensional endomorphisms, fractalization, bifurcations.

The family T generates different mechanisms of basin boundary fractalization when the parameter c is fixed with γ varying $\gamma < 0$, $\gamma = 0$, $\gamma > 0$. The paper study is limited to one of them, that is, we fix $c = -0.15$. In this case only one attractor exists, a stable fixed point, whose basin of attraction, say B, remains simply connected. The complementary set of the closure $\overline{B}$ of B gives the plane region B_∞, the points of which have divergent trajectories.

The main feature of the map (1) is that for $\gamma = 0$, in the invariant half-plane $\Pi_- = \{(x, y) : y < 0\}$, there exists a semiconjugacy between the map T and the complex quadratic map Z ($z' = z^2 - c$), c being a real parameter, $z = x + jy$, $j^2 = -1$. That is a semiconjugacy in Π_- between T and the real two-dimensional map T_Z

$$T_Z : \begin{cases} x' = x^2 - y^2 - c \\ y' = 2xy \end{cases} \tag{2}$$

which allows to get a boundary whose complex structure is particular and well known. This basic property permits to identify the routes to a fractal basin boundary, and the fractalization type, showing some interesting bifurcations governing the transition *smooth* $\leftrightarrow$ *fractal*, and the one *fractal* $\leftrightarrow$ *half fractal*, of the frontier ∂B. Note that, following Mira *et al.* 1996b, we call "*half fractal*" a frontier made up of infinitely many smooth arcs having a fractal limit set. As shown in section 4, the transition *fractal* $\leftrightarrow$ *half fractal* in our family T is associated with the *Riemann foliation* of the phase plane. This is not the only possible mechanism, because such a transition may also occur via the appearance on the fractal frontier of smooth arcs not directly related to the plane foliation, but associated with the stable set of some saddle cycles, or with the unstable set of repelling nodes or foci, not directly related with the critical curves of the map (examples may be found in Narayaninsamy 1992, and in Mira *et al.* 1996b). In the case of the family T this transition also gives rise to smooth arcs, belonging to the stable set of some saddle cycle, and interfering in an initially "fully fractal" basin boundary. The basic difference lies in a bifurcation of the critical curve LC and thus in a qualitative change of the plane foliation.

The plan of the work is as follows. Section 2 is devoted to some introductory properties and to the plane foliation. Section 3 deals with the transition of basin boundary from smooth to fractal as the parameter γ decreases in the interval $1 > \gamma \geq 0$, in the particular case corresponding to $c = -0.15$. As said above the only attractor is a stable fixed point, its basin B being a simply connected basin. It will be shown that the route to fractalization of the basin boundary ∂B occurs via sequences of local and global bifurcations of the cycles located on ∂B. Such a sequence of bifurcations has the fractal "*box-within-a-box*" structure associated with the cycles belonging to ∂B. That is, the bifurcations sequences are strictly related to the one generated by the one-dimensional Myrberg's map $x' = x^2 - c$, $-1/4 \leq c \leq 2$ (topologically conjugated with the standard

logistic map), as described in Gumowski & Mira 1980 and Mira 1987 (see also Mira *et al.* 1996b). Section 4 deals with the transition *fractal* $\leftrightarrow$ *half fractal* of the frontier ∂B of the basin B. It will be shown that the basic mechanism is related with the phase plane foliation which gives rise to infinitely many smooth arcs on the frontier ∂B, having as limit set a strange repellor Λ.

2 Some properties of the map T.

For the map T the x-axis is a trapping set and the restriction of T to that axis reduces to the well known Myrberg's map (conjugate to the logistic map)

$$x' = x^2 - c$$

Thus, at $c = -0.25$ a saddle-node bifurcation occurs, and for $c > -0.25$ T admits two fixed points on the x-axis, say P^* and Q^* :

$$P^* = \left(\frac{1-\sqrt{1+4c}}{2},\ 0\right) \quad , \quad Q^* = \left(\frac{1+\sqrt{1+4c}}{2},\ 0\right).$$

The fixed point Q^*, which corresponds to the repelling fixed point of the Myrberg's map, is always unstable for the map T, a saddle or a repelling node as it is easy to see from the Jacobian matrix

$$J(x,y) = \begin{bmatrix} 2x & 1 \\ 8xy & \gamma + 4x^2 \end{bmatrix}. \tag{3}$$

The eigenvalues of $J(Q^*)$ are $S_1(Q^*) = 1 + \sqrt{1+4c}$ with eigendirection $r_1 = (1,0)$ and $S_2(Q^*) = \gamma + \left(1+\sqrt{1+4c}\right)^2$ with eigendirection $r_2 = (-1, 1+\sqrt{1+4c})$. The eigenvalues of $J(P^*)$ are $S_1(P^*) = 1 - \sqrt{1+4c}$ with eigendirection $r_1 = (1,0)$ (i.e. it is the eigenvalue of the restriction of T to the $x-$axis) and $S_2(P^*) = \gamma + \left(1-\sqrt{1+4c}\right)^2$ with eigendirection $r_2 = (1, \sqrt{1+4c} - 1)$.

Summarizing, in the interval $-1/4 < c < 3/4$ the fixed point P^* is attracting for the restriction on the $x-$axis, and a flip bifurcation ($S_1 = -1$) occurs at $c = 3/4$. No other cycles exist on the $x-$axis besides the two fixed points P^* and Q^*. For $3/4 < c < c_{1s} \simeq 1.401155189$ the restriction of T to the x-axis generates period 2^i cycles for any i, c_{1s} being obtained when $i = \infty$. The interval $c_{1s} < c < c_1^* = 2$ leads to the generation of period-$k2^i$ cycles, $k = 3, 4, 5, ..., i = 0, 1, 2, 3, ...$ For $c = c_1^* = 2$ all the possible cycles and their limit set have been created on the x-axis. These cycles and their increasing rank preimages constitute a real set (E), occupying the whole interval $[-2 \le x \le 2]$, the derived set (set of limit points) (E') of which is *perfect*. The preimages of any point of (E) are everywhere dense on (E'). From this situation the bifurcations inside $c_{(1)0} = -1/4 \le c \le c_1^*$ have a fractal structure of box-within-a-box type (Gumowski & Mira 1980, Mira 1987, Mira et al. 1996b).

Moreover, at $\gamma = 1$ another saddle-node bifurcation occurs, so that for $\gamma < 1$, the map T admits two more fixed points:

$$\begin{aligned} R^* &= \left(-\frac{\sqrt{1-\gamma}}{2},\ c - \frac{1-\gamma}{4} - \frac{\sqrt{1-\gamma}}{2}\right) \\ S^* &= \left(\frac{\sqrt{1-\gamma}}{2},\ c - \frac{1-\gamma}{4} + \frac{\sqrt{1-\gamma}}{2}\right) \end{aligned}$$

At the bifurcation value $\gamma = 1$ the two fixed points $R^* = S^* = (0, c)$ belong to the curve LC_{-1} of rank-one merging preimages defined above (the Jacobian determinant $|J(x,y)| = 0$) with multipliers (eigenvalues) $S_1 = 1$ and $S_2 = 0$. Then the local stability analysis of the fixed points is straightforward. We note that for $c = \frac{1-\gamma}{4} - \frac{\sqrt{1-\gamma}}{2}$ and $0 < \gamma < 1$ (resp. $\gamma < 0$), the fixed point S^* merges with P^* (resp. Q^*) with the eigenvalue $S_2(P^*) = +1$ (resp. $S_2(Q^*) = +1$), whereas for $c = \frac{1-\gamma}{4} + \frac{\sqrt{1-\gamma}}{2}$ the fixed point R^* always merges with P^*, with $S_2(P^*) = +1$.

The map T is symmetric with respect to the axis $x = 0$, i.e. $T(x,y) = T(-x,y)$. This means that points symmetric with respect to the y-axis have the same asymptotic behavior, giving rise to the same trajectory, then the basins are symmetric sets. Moreover when the preimages of a point P of the phase plane exist, by pair they are symmetric with respect to the y-axis.

Being T a noninvertible map, the Riemann foliation of the phase plane is at the origin of some fundamental properties of the solutions generated by this map. The Jacobian determinant $|J(x,y)| = 2x\gamma + 8x^3 - 8xy$, vanishes on two curves, the $y-$axis and a parabola, constituting the set LC_{-1}, $LC_{-1} = L^a_{-1} \cup L^b_{-1}$ (see Figure 1a) where

$$L^a_{-1}: \ x = 0 \quad , \quad L^b_{-1}: \ y = \frac{\gamma}{4} + x^2 \tag{4}$$

The rank-one image of these two curves gives the critical curve LC, made up of two branches, $LC = L^a \cup L^b$ (see Figure 1, b,c,d) where

$$L^a: \ y = \gamma(x + c) \quad , \quad L^b: \ \begin{cases} y = \left(x + c + \frac{\gamma}{4}\right)^2 \\ x \ge \frac{\gamma}{4} - c \end{cases} \tag{5}$$

In the phase plane the critical curve LC separates regions Z_i, each point of which has i rank-1 preimages, $i = 0, 2, 4$. These regions are bounded by the following arcs of LC:

- a straight line L^a with positive (resp. negative) slope if $\gamma > 0$ (resp. $\gamma < 0$) intersecting the x-axis in the point $(-c, 0)$ ($x = -c$ is the rank one critical value of the Myrberg's map),

- a branch of parabola L^b, tangent to L^a in the cusp point $C = \left(-c + \frac{\gamma}{4}, \frac{\gamma^2}{4}\right)$, and for $\gamma < 0$ L^b is tangent to the x-axis in its vertex $V = \left(-c - \frac{\gamma}{4}, 0\right)$.

In the particular case $\gamma = 0$, L^a reduces to the x-axis and is tangent to the L^b in the point $(-c, 0)$.

The region Z_0 always exists, and Z_4 becomes wider and wider as the parameter γ decreases. The region Z_0 is a subset of $\Pi_+ = \{(x, y) : y > 0\}$ if $\gamma \leq 0$, whereas the region Z_4 is a subset of Π_+ if $\gamma \geq 0$ (see Figure 1).

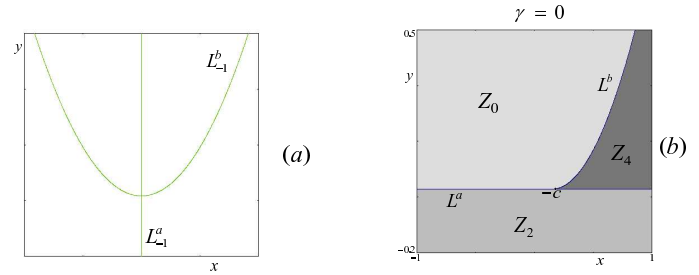

Figure 1

Figure 1: Critical curves and Z_i $(i = 0, 2, 4)$ regions. **(a)** $LC_{-1} = L^a_{-1} \cup L^b_{-1}$. **(b)** $LC = L^a \cup L^b$ in the case $\gamma = 0$. **(c)** $LC = L^a \cup L^b$ in the case $\gamma > 0$. **(d)** $LC = L^a \cup L^b$ in the case $\gamma < 0$.

The equation of L^b shows that it is a "double" arc. This is indeed a non standard property, associated with a particular foliation of the plane. In fact, the map T in (1) corresponds to a non generic case of the map

$$T_\varepsilon : \begin{cases} x' = x^2 + y - c \\ y' = \gamma y + 4x^2 y + \varepsilon x \end{cases}$$

when $\varepsilon = 0$. The map T_ε is of so-called type $Z_0 - Z_2 < Z_4$ (following the notation used in Mira *et al.* 1996a, Mira *et al.* 1996b), the symbol $<$ denoting the existence of a *cusp*

point on the critical curve corresponding to a cape of Z_4 "penetrating" into Z_2. The non genericity of the map T in the case $\varepsilon = 0$ corresponds to a bifurcation value for LC, which exhibits a "double" arc resulting from the merging of two arcs of the critical set LC, as shown in the qualitative figures of Figure 2.

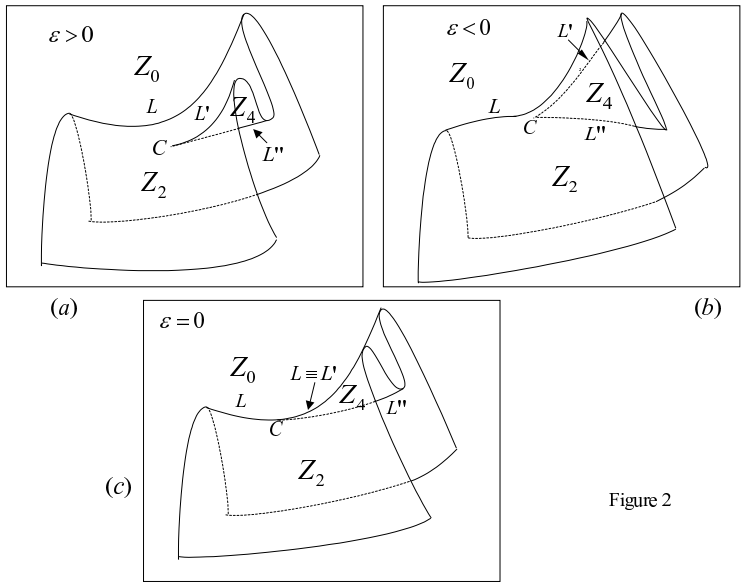

Figure 2

Figure 2: Qualitative Riemann foliation of the plane induced by the maps T_ε and T.

This paper essentially deals with the dynamic properties of the map T because it is simpler than T_ε (in fact, as we shall see below, all the inverses of T can be given explicitly), but mainly because for $\gamma = 0$ the map T is topologically semiconjugated to the complex quadratic map in $\Pi_- = \{(x, y) : y < 0\}$

The inverses of a point $p = (u, v)$, for the map T, are obtained by solving with respect to (x, y) the system $u = x^2 + y - c$, $v = \gamma y + 4x^2 y$. Any point $p = (u, v)$ not belonging

to the region Z_0 has the following inverses:

$$T_{d_R}^{-1}(u,v) = \left(\sqrt{\xi}\ ,\ u+c-\xi\right)\ ,\ T_{d_L}^{-1}(u,v) = \left(-\sqrt{\xi}\ ,\ u+c-\xi\right) \qquad (6)$$

$$\text{where}\ \ \xi = \frac{1}{2}\left(u+c-\frac{\gamma}{4}+\sqrt{\left(u+c+\frac{\gamma}{4}\right)^2-v}\right)$$

while any point $p=(u,v)$ belonging to the region Z_4, besides the two inverses given above, also has the following two inverses:

$$T_{u_R}^{-1}(u,v) = (\sqrt{\eta}\ ,\ u+c-\eta)\ ,\ T_{u_L}^{-1}(u,v) = (-\sqrt{\eta}\ ,\ u+c-\eta) \qquad (7)$$

$$\text{where}\ \ \eta = \frac{1}{2}\left(u+c-\frac{\gamma}{4}-\sqrt{\left(u+c+\frac{\gamma}{4}\right)^2-v}\right)$$

Clearly the positions of the rank-one preimages of a point p depend on the value of the parameters. However, for $\gamma \leq 0$ any point of Π_- has at least two preimages (exactly two if $\gamma = 0$), and two of these preimages, given by T_d^{-1} in (6), always belong to Π_-, one on the left and one on the right of the $y-$axis (L_{-1}^a). Moreover a point p belonging to $\Pi_- \cap Z_4$, has two more preimages, given by T_u^{-1} in (7), which belong to Π_+. The fact that for $\gamma \leq 0$ any point of Π_- has at least two preimages in Π_- implies the existence of infinitely many periodic points in this half-plane. Indeed after n iterations each point of Π_- gives rise to at least 2^n points preimages of rank-n, an arborescent sequence tending with $n \to \infty$ toward a limit set SR of strange repeller type. The set SR is made up of infinitely many unstable cycles and their limit when their period tends toward infinity. This means that all the possible cycles, of any period, and, for each period, of any possible rotation sequence (i.e. the permutation type of the cycle points), exist on the left and on the right of the $y-$axis (although not all belonging to the frontier of the immediate basin).

Furthermore, we can observe that if $\gamma > 0$ then the half-planes Π_+ and Π_- are both trapping, being $T(\Pi_+) \subseteq \Pi_+$ and $T(\Pi_-) \subseteq \Pi_-$. If $\gamma < 0$ such a property does not hold, whereas for $\gamma = 0$ the negative half-plane is invariant ($T(\Pi_-) = \Pi_-$) and the positive one is still trapping. As shown in section 4, the fact that Π_+ is not trapping in the case $\gamma < 0$ gives rise to a half fractal boundary for the basin B also in that region of the plane.

As stated above, for $\gamma = 0$ the map T is topologically semiconjugated to the complex quadratic map Z given in (2), in the negative half-plane Π_-. In fact in this case the map T with $\gamma = 0$, say $T_{\gamma=0}$, reduces to the map already considered in Agliari *et al.* 2003 (with $\gamma = \beta - 1$). We briefly recall the proof given there. The following equality holds $T_{\gamma=0} \circ h = h \circ Z$, where $h(x,y) = (x,-y^2)$. Indeed $T_{\gamma=0} \circ h(x,y) = T_{\gamma=0}(x,-y^2) = (x^2-y^2-c,-4x^2y^2)$, $h \circ Z(x,y) = h(x^2-y^2-c,2xy) = (x^2-y^2-c,-4x^2y^2)$. This property is essential because it permits an easier study of the structure of the boundary ∂B, when the transitions from smooth to fractal (section 3) and from fractal to half

fractal (section 4) occur, as the parameter γ decreases from positive values to negative ones.

3 Transition of the boundary from smooth to fractal

Let $c = -0.15$ be the fixed value of the parameter c. The only singular points of T on the $x-$axis are the fixed points, P^* with $0 < S_1(P^*) < 1$, and Q^* with $S_1(Q^*) > 1$, no other cycle exists on this axis for any value of $\gamma < 1$. When $\gamma_{b1} \simeq 0.86491 > \gamma \geq 0$ the fixed point P^* is the unique attractor of the map T. All the other fixed points are unstable and belong to the boundary of the basin $B = B(P^*)$. In particular, the point R^* belongs to the negative half-plane Π_-.

At $\gamma = 1$ P^* is a saddle of T, transversely repelling. The parameter $\gamma = 1$ corresponds to a saddle-node bifurcation, for which the fixed points R^* and S^* merge in the point $(0,c)$ of the $x-$axis. For $1 > \gamma > \gamma_{b1} \simeq 0.86491$, R^* is a saddle and S^* a stable node of T. The bifurcation value $\gamma = \gamma_{b1}$ is such that P^* and S^* merge with $S_2 = \gamma + \left(1-\sqrt{1+4(-0.15)}\right)^2 = +1$, exchanging their stability, so that for $0 \leq \gamma < \gamma_{b1}$ P^* is the only attractor of T, and S^* a saddle belonging to Π_+. Figure 3 shows the basin B of P^* which is simply connected. Moreover $\partial B_+ = \partial B \cap \Pi_+$ is smooth, including the stable set $W^s(S^*)$ of the saddle S^* and no other cycle of T.

In the parameter interval $0 \leq \gamma < \gamma_{b1}$ the structure identification of the basin boundary arc $\partial B_- = \partial B \cap \Pi_-$ is highly facilitated by the considerations which follow.

-(a) Numerical simulations show that B remains a simply connected basin for the values of γ considered in this work.

-(b) These simulations show that the critical arc L^a intersect ∂B_- in a critical point (in the Julia-Fatou sense) C^a, $C^a = \partial B_- \cap L^a$ separating an arc Z_0 from a Z_2 one, for the restriction T_{RB} of T to ∂B_-. Its rank one preimage $C_{-1}^a \in L_{-1}^a$ plays the role of an extremum for a one-dimensional quadratic map, and T_{RB} behaves as a one-dimensional map defined by a function having only one extremum and a negative Schwarzian derivative. Then when γ varies in the interval $0 \leq \gamma < \gamma_{b1}$ T_{RB} generates on ∂B_- a fractal bifurcation structure of box-within-a-box type related to a one-dimensional quadratic map (for example the map $x' = x^2 - c$ mentioned above), because C^a is the unique critical point on ∂B_-. In particular the cycles tables of Gumowski & Mira 1980 permit to forecast the cycles with their rotation sequence which can be found on ∂B_-. So the fixed point $R^* \in \partial B_-$ remains a saddle in an interval $\gamma_{b2} \leq \gamma < \gamma_{b1}$, equivalent to the interval $-1/4 < c \leq 3/4$ related to $x' = x^2 - c$.

-(c) For $\gamma = 0$, in the negative half-plane Π_-, T is topologically semiconjugated to the one-dimensional complex quadratic map Z, given in (2) as a two-dimensional real map T_Z. When $c = -0.15$ T_Z has a fixed point as unique attractor. In the (x,y) plane its basin boundary, nowhere smooth, is the Julia set made up of all the possible cycles generated by T_Z and their increasing rank preimages. These points constitute a real set (E), occupying the whole boundary, the derived set (set of limit points) (E') of which is *perfect*. The preimages of any point of (E) are everywhere dense on (E'). It results that

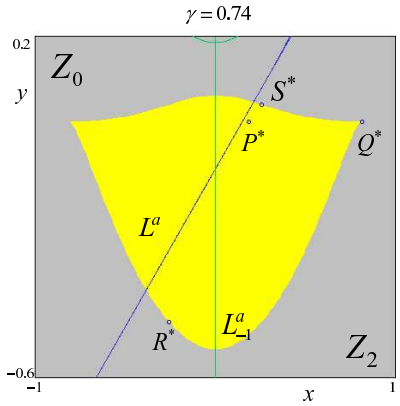

Figure 3

Figure 3: The simply connected basin of attraction B of P^* (white points). The grey points belong to B_∞.

∂B_- is nowhere smooth, and fully occupied by the sets (E) and (E'). This means that $\gamma = 0$ is the limit bifurcation value γ_1^* for the creation of new cycles by T_{RB}, equivalent to the value $c_1^* = 2$ defined above for the map $x' = x^2 - c$.

-(d) The parameter interval $\gamma_{b1} > \gamma \geq \gamma_1^* = 0$ has the same fractal bifurcation structure of box-within-a-box type related to a one-dimensional quadratic map $x' = x^2 - c$. For the restriction T_{RB} on ∂B_- only one attractor exists (a saddle for T).

From the situation of Figure 3, where the boundary ∂B_- includes only the stable set of the saddle R^*, the above points permits to understand what occurs when γ decreases from $\gamma_{b1} \simeq 0.86491$ The saddle R^* turns into a repelling node at $\gamma = \gamma_{b2} \simeq 0.73585$ with $S_1 = -1$ (and $S_2 > 1$), giving rise to a cascade of period 2^i cycles on ∂B_-, $i = 1, 2, 3, ...$, initially saddles then turning into repelling nodes when the multiplier S_1 decreases crossing through -1. When $i = \infty$ the limit of this cascade by period doubling is attained for $\gamma = \gamma_{1s}$. It is equivalent to the parameter $c = c_{1s} \simeq 1.401155189$ of the map $x' = x^2 - c$. Moreover $\gamma = \gamma_{1s}$ is a limit of a sequence of homoclinic bifurcation

values $\gamma_{2^i}^* < \gamma_{2^{i+1}}^* ... < \gamma_{1s}$, $i = 1, 2, 3, ...$, $\gamma_{1s} = \lim_{i\to\infty} \gamma_{2^i}^*$. The position of the critical points $C_n^a = T^n(C^a) = \partial B_- \cap L_n^a$, $L_n^a = T^n(L^a)$, with respect to a period 2^i cycle, $i = 0, 1, 2, 3, ...$, born from the above period doubling cascade, permits to approach the $\gamma_{2^i}^*$ values by successive trials. For $\gamma = \gamma_{2^i}^*$ the above unstable period 2^{i-1} cycle merges with a rank $2^i + 1$ critical point $C_{2^i}^a = T^{2^i}(C^a)$.

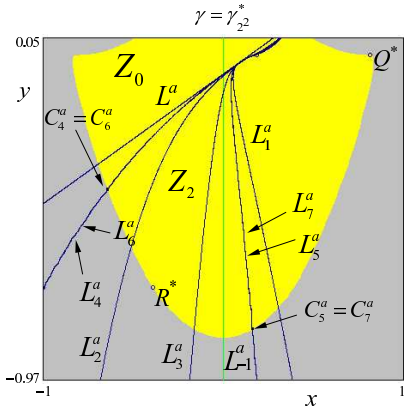

Figure 4

Figure 4: Enlargement of the basin B at $\gamma = 0.3865$.

Figure 4 shows the situation when $\gamma = \gamma_{2^2}^* \simeq 0.3865$. At the figure scale the critical arcs L_4^a and L_6^a (resp. L_5^a and L_7^a) seem merging. It is not the case they intersect on ∂B_- at a point of the period two cycle born from the period doubling of R^*. Figures 5 a,b,c show what occurs for $\gamma = \gamma_{2^1}^* \simeq 0.3242$, $\gamma_{2^1}^* < \gamma < \gamma_{2^2}^*$, and $0 = \gamma_1^* < \gamma < \gamma_{2^1}^*$.

The bifurcation values $\gamma = \gamma_{2^i}^*$ are those at which the first homoclinic orbits of the expanding cycles of period 2^i, born from a flip bifurcation, appear. That is, they correspond to the values at which such cycles become snap back repeller (following Marotto, 1978). As an example let us briefly comment this in relation with the snap back repeller (*sbr* for short) bifurcation of the fixed point R^*, at $\gamma = \gamma_{2^1}^* \simeq 0.3242$,

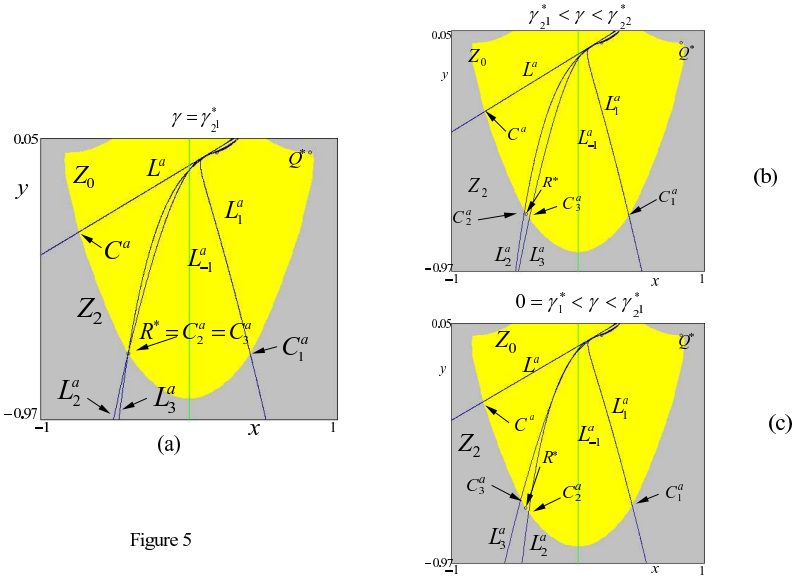

Figure 5

Figure 5: (a) Enlargement of the basin B at $\gamma = 0.3242 \simeq \gamma^*_{2^1}$. (b) Enlargement of the basin B at $\gamma = 0.33 > \gamma^*_{2^1}$. (c) Enlargement of the basin B at $\gamma = 0.315 < \gamma^*_{2^1}$.

but clearly similar behaviours occurs at any other bifurcation value $\gamma^*_{2^i}$, associated with the other cycles of period 2^i. In Figure 6a just above the bifurcation value $\gamma^*_{2^1}$, the two rank-1 preimages of the fixed point R^* are the point itself and $R^{d_R}_{-1}$ on the right of L^a_{-1} belonging to Z_2. Then the preimages of $R^{d_R}_{-1}$ consist of two points, $R^{d_R d_R}_{-2} = T^{-1}_{d_R}(R^{d_R}_{-1})$ which belongs to Z_2, while $R^{d_R d_L}_{-2} = T^{-1}_{d_L}(R^{d_R}_{-1})$ is in Z_0. And so on, all the preimages $T^{-k}(R^*)$ of any rank k of the fixed point R^* consist of one point on the right belonging to Z_2 and of one point in Z_0. In particular, no homoclinic orbit of R^* can exist, so that the fixed point R^* is expanding but not *sbr*.

In Figure 6a we can see that the point $R^{d_R d_L}_{-2}$ is quite close to the boundary of the region Z_0 and the merging occurs when the point $R^{d_R d_L}_{-2}$ becomes the critical point C^a, at the bifurcation value $\gamma = \gamma^*_{2^1}$, which is the *sbr* bifurcation. As shown in Gardini 1994, at the *sbr* bifurcation of an expanding fixed point (node or focus) all the homoclinic orbits are critical. An example, the sequence of points $T^{-m}_{d_L}\left(R^{d_R}_{-1}\right) \to R^*$ as $m \to \infty$, is shown

Figure 6

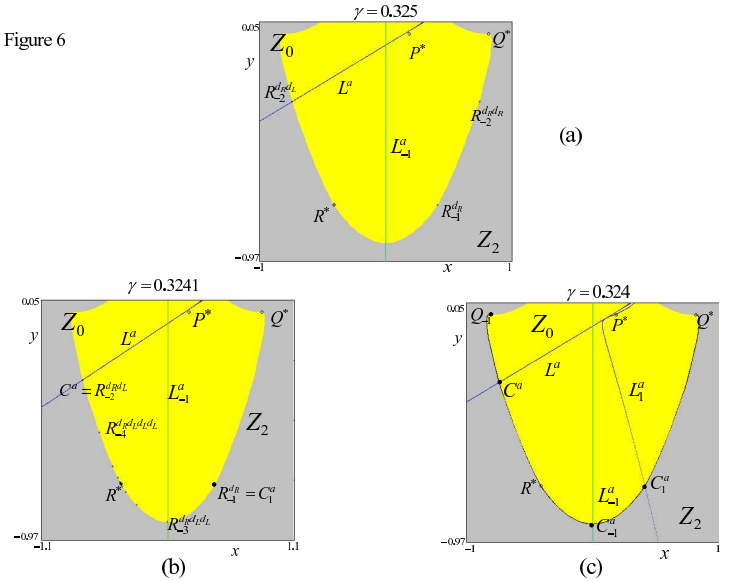

Figure 6: (a) Enlargement of the basin B at $\gamma = 0.325 > \gamma^*_{2^1}$,.just above the *sbr* bifurcation value. (b) Enlargement of the basin B at $\gamma = 0.3241 \simeq \gamma^*_{2^1}$, the *sbr* bifurcation value, a critical homoclinic orbit is shown. (c) Enlargement of the basin B at $\gamma = 0.324 < \gamma^*_{2^1}$, soon after the *sbr* bifurcation value.

in Figure 6b, but any homoclinic orbit of R^* includes the critical points $R^{d_R d_L}_{-2} = C^a$ and $R^{d_R}_{-1} = C^a_1$. For $\gamma < \gamma^*_{2^1}$ (see Figure 6c) the point $R^{d_R d_L}_{-2}$ belongs to Z_2 and infinitely many noncritical homoclinic orbits of R^* exist. As an example, the sequence of points $T^{-m}_{d_L}\left(R^{d_R}_{-1}\right) \to R^*$ as $m \to \infty$ gives now a noncritical homoclinic orbit of R^*, and infinitely many other can be obtained by using $T^{-m}_{d_L}(X)$ being X a preimage of some rank of R^*. We note that at the *sbr* bifurcation these preimages are dense on the arc of frontier ∂B_- between the points $C^a = L^a \cap \partial B_-$ and $C^a_1 = T(C^a)$, which bound a chaotic interval, and all these preimages still exist after the bifurcation (see Figure 6c).

A similar behaviour occurs to the preimages of the 2-cycle as γ crosses through the value $\gamma^*_{2^2}$ (see Figure 5a), which is the *sbr* bifurcation of the 2-cycle.

In the interval $\gamma^*_{2^1} \le \gamma < \gamma_{b2}$ cycles with an odd period do not exist. They appear

(with other cycles of even period) from bifurcations in the interval $\gamma_1^* \le \gamma < \gamma_{2^1}^*$. More details on the fractal bifurcation structure of box-within-a-box type, and so on the one related to the interval $\gamma_{b1} > \gamma \ge \gamma_1^* = 0$, can be found in Gumowski & Mira 1980, Mira 1987, Mira et al. 1996b.

When γ decreases from $\gamma = \gamma_{b2}$, with $c = -0.15$, the route to fractalization of ∂B_- occurs from the incorporation to this boundary of "more and more" sequences of infinitely many unstable cycles of increasing period created by the above fractal bifurcation structure. For the restriction of T to ∂B_- they constitute a strange repeller leading to a chaotic transient toward the attractor of this restriction. For $\gamma = \gamma_1^* = 0$, ∂B_- has the fractal properties as the ones generated by the complex map $z' = z^2 + 0.15$ (two enlargements are shown in Figure 7).

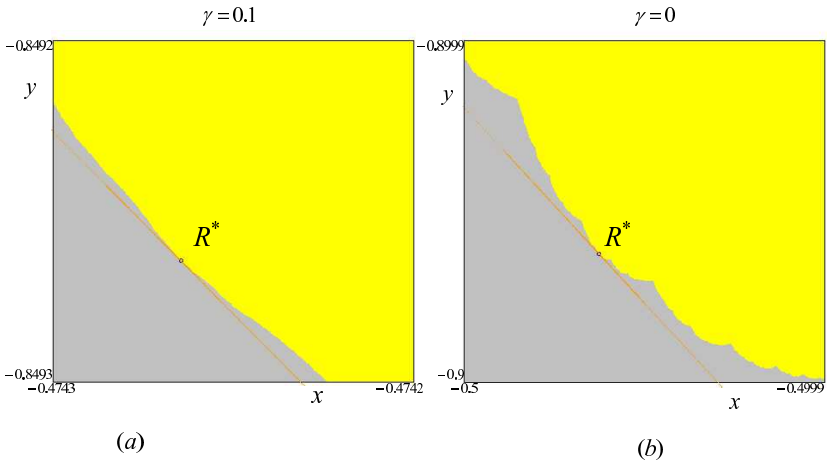

Figure 7

Figure 7: Enlargement of the frontier∂B_- near the fixed point R^*. (a): in the case $\gamma > 0$, and the direction of an eigenvector is also shown. (b): in the case $\gamma = 0$.

We remark that this property holds only at the bifurcation value $\gamma = 0$ (see Figure 7b), as for any positive value of γ the frontier ∂B_- is smooth, although it may be with

complex dynamics on it (as shown in Figure 7a), while for any negative value of γ the frontier ∂B_- is half fractal (with complex dynamics on it) as we shall see in the next section.

4 Transition of the boundary from fractal to half fractal

In the previous section we have studied the transition of the frontier ∂B_- from smooth to fractal, which is obtained for positive values of γ decreasing toward 0. In this section we consider negative values of the parameter γ and we shall see the transition of a fractal boundary to an half fractal one.

We recall that for $\gamma < 0$ the two half planes are not trapping, i.e. there are points belonging to Π_- which are mapped in Π_+ and *vice versa*, as we can see from the preimages of T given in (6) and in (7). However, the main feature of the map, whichever is the value of c, which persist for $\gamma < 0$ is that any point belonging to Π_- has the two preimages given by (6) which belong to Π_-. Thus all the possible cycles existing in Π_- for $\gamma = 0$ (when the set is *perfect*) persists also for $\gamma < 0$, and belong to ∂B_-. All the points of the cycles existing in $\partial B(A)_-$, their preimages of any rank and their limit points form a set which we denote by Λ, which is an invariant set with Cantor like structure, that is a strange repeller $\Lambda \subset \partial B_-$.

The transition to half fractal boundary which occurs for $\gamma < 0$ is due to the Riemann foliation of the plane. In fact, as γ decreases the critical curve L^a has a negative slope (see Figure 1d) which causes the appearance of a portion of region Z_2 in Π_+ to the left of the vertical axis, and the appearance of a portion of region Z_4 in Π_- to the right of the vertical axis. The preimages of the portion of frontier in these zones are responsible of the appearance of smooth arcs on the frontier of B and of points of non smoothness in ∂B_+.

We always consider $c = -0.15$. The attracting set of the map, for values of γ just below 0, is always the fixed point P^*, belonging to the x-axis, so that $B = B(P^*)$. All the other fixed points of T belong to ∂B as shown in Figure 8a.

In the enlargement in Figure 9a we see the smooth arc, called ψ, which is the boundary of $B \cap Z_2 \cap \Pi_+$, bounded by the points Q_{-1} and q, which is responsible of the smooth parts belonging to Π_-. Considering the preimages of this arc, given by the two inverses in (6), we get a smooth arc crossing L^a_{-1}. Due to the fact that these preimages belong to the region $Z_2 \cap \Pi_-$ we can state that all the possible 2^k (for any $k \ge 1$) preimages of any rank exist in Π_- and these preimages have as limit points all the points of the strange repellor $\Lambda \subset \partial B_-$. In the enlargement of Figure 8b we see arcs accumulating in the fixed point R^* which is a cusp point (having eingenvalues $S_1 < -1$, $S_2 > 1$ and $|S_1| > S_2$), and a non-smooth point of the frontier (as well as any other point of Λ). Thus the frontier ∂B_-, however small is γ, is now almost smooth, as it is smooth except for a set of points of zero Lebesgue measure, which belong to a strange repellor Λ, that is: the frontier ∂B_- is half fractal.

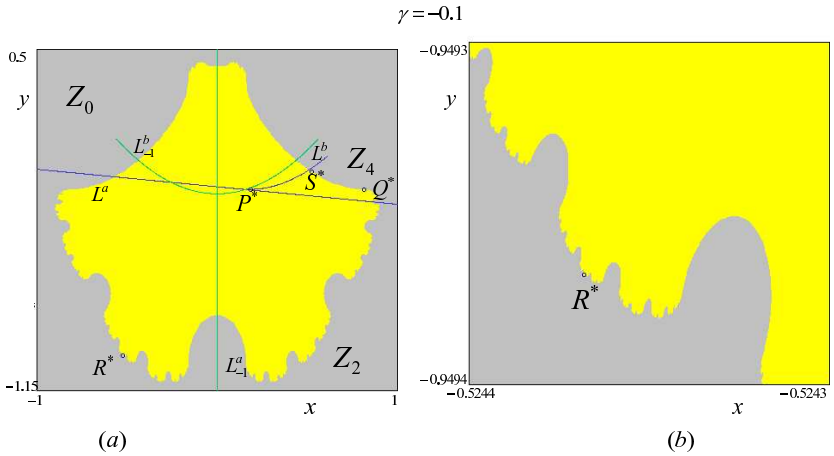

Figure 8

Figure 8: (a) The connected set $B = B(P^*)$, in the case $c = -0.15$ and γ just below 0. (b) Enlargement of ∂B_- near the fixed point R^* evidencing the half fractal structure.

A different sequence of preimages are associated with the other arc of frontier, ϕ, shown in the enlargements in Figure 8b, which is the boundary of $B \cap Z_4 \cap \Pi_-$, bounded by the points Q^* and p. This arc ϕ includes a part of the half fractal structure existing in ∂B_- (as explained above), and is responsible of the non-smooth points in Π_+, which belong to the two preimages of this arc obtained by the two inverses in (7). Due to the fact that these preimages belong to the region Z_0 no further preimages are obtained in Π_+.

5 Conclusions

In this paper we have described two particular routes to fractal basin boundary occurring in a two-dimensional noninvertible family of maps depending on two parameters, c and γ. The peculiar fact is that for $\gamma = 0$ the family is topologically semiconjugated to the

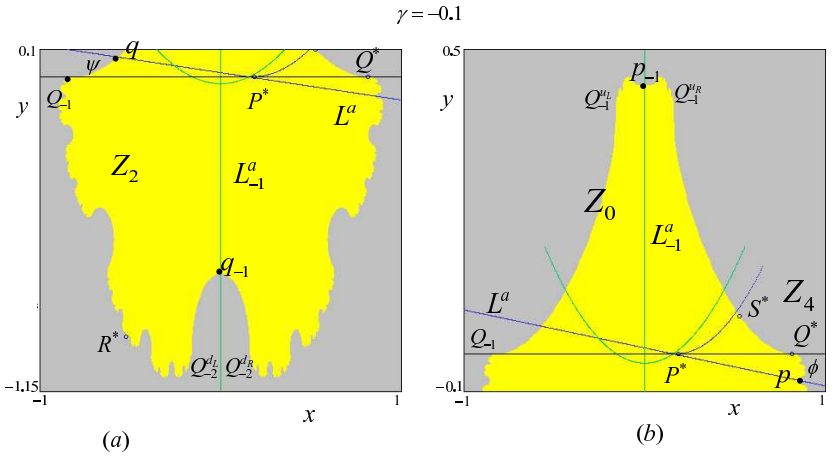

Figure 9

Figure 9: (a) The smooth arcs in ∂B_- are the 2^k preimages of the arc ψ, boundary of $B \cap Z_2 \cap \Pi_+$, with extrema the points Q_{-1} and q. Such preimages accumulate on a strange repellor. (b) Points of non-smoothness in ∂B_+: they belong to the rank-1 preimages of the arc ϕ, boundary of $B \cap Z_4 \cap \Pi_-$, with extrema the points Q^* and p.

complex quadratic map Z. To simplify the analysis we have considered only the case $c = -0.15$, and the variation of the parameter γ permits a full identification of two phenomena. On one side, for decreasing positive values of γ, we have described one of the possible bifurcation mechanisms leading to the fractalization of a basin boundary from a smooth situation. On the other side, for negative values of γ, decreasing from 0, we have seen the transition of a basin boundary from fractal to half fractal. The main peculiarity occurring in the case $\gamma > 0$ is that the bifurcations occurring at the periodic points on the boundary ∂B_- have the fractal structure of *box-within-a-box* type, i.e. are topologically conjugated to those occurring in the one-dimensional Myrberg's map $x' = x^2 - c$. The main peculiarity occurring in the case $\gamma < 0$ is that the whole strange repellor Λ existing on ∂B_- for $\gamma = 0$ still persists on ∂B_- for negative values of γ.

Certainly all the possible mechanisms of transitions of a *smooth* boundary *to* a *fractal*

one, or transition from a *fractal* boundary to an *half fractal* one, are not covered by this only example. We may expect that other mechanisms may be observed when we fix different values for the parameter c, and this will be the object of further investigations.

Acknowledgments. This work has been performed under the activity of the national research project "Dynamic models in economic and finance: complex dynamics, disequilibrium, strategic interaction", MIUR, Italy.

REFERENCES

Abraham R., Gardini L. and Mira C., 1997. *Discrete Dynamical Systems in Two Dimensions*. Springer-Verlag, Telos, New York.

Agliari A., Gardini L. and Mira C., 2003. "On the fractal structure of basin boundaries in two-dimensional noninvertible maps", *Int. Journal of Bifurcations and Chaos*, *13 (7)*, 1767 - 1785.

Gardini L., 1994. "Homoclinic bifurcations in n-dimensional endomorphisms, due to expanding periodic points", *Nonlinear Analysis, Theory, Methods & Applications*, 23(8), 1039 - 1089.

Gumowski I. and Mira C., 1980. *Recurrences and discrete dynamic systems*. Lectures Notes in Mathematics 809, Springer-Verlag.

Marotto J.R., 1978. "Snap-back repellers imply chaos in R^n", *J. Math. Analysis Applic*, 63, 199 - 223.

Mira C., 1987. *Chaotic Dynamics*. World Scientific, Singapore.

Mira C., Fournier-Prunaret D. , Gardini L., Kawakami H. and Cathala J.C., 1994. "Basin bifurcations of two-dimensional noninvertible maps. Fractalization of basins", *Int. Journal of Bifurcation and Chaos*, 4(2), 343 - 381.

Mira C., Carcasses J.P. , G. Millérioux. and Gardini L. , 1996a. "Plane foliation of two dimensional noninvertible maps", *Int. Journal of Bifurcation and Chaos*, 6(8) pp. 1439 - 1462.

Mira C., Gardini L. , Barugola A. and Cathala J. C., 1996b. *Chaotic Dynamics in Two-dimensional Noninvertible Maps*. World Scientific, Singapore.

Narayaninsamy T., 1992. "Contribution à l'etude de l'itération fractionnaire et à celle des endomorphismes bidimensionnels". These de Doctorat de l'Université Paul Sabatier N. 1295, Toulouse.

Anna Agliari
Catholic University of Milan
I - 20123 Milan, Italy
e-mail: anna.agliari@unicatt.it

Laura Gardini
Istituto di Scienze Economiche, University of Urbino
I - 61029 Urbino, Italy
e-mail: *gardini@uniurb.it*

Christian Mira
19 rue d'Occitanie,
F - 31130 Quint Fonsegrives, France
and Istituto di Scienze Economiche, University of Urbino
e-mail: *c.mira@free.fr*